Long-lived quantum coherence and non-Markovianity of photosynthetic complexes

Hong-Bin Chen,[1] Jiun-Yi Lien,[1,2] Chi-Chuan Hwang,[2] and Yueh-Nan Chen[1,*]

[1]*Department of Physics and National Center for Theoretical Sciences, National Cheng Kung University, Tainan 701, Taiwan*

[2]*Department of Engineering Science and Supercomputing Research Center, National Cheng Kung University, Tainan 701, Taiwan*

(Received 4 December 2013; published 29 April 2014)

Long-lived quantum coherence in photosynthetic pigment-protein complexes has recently been reported at physiological temperature. It has been pointed out that the discrete vibrational modes may be responsible for the long-lived coherence. Here, we propose an analytical non-Markovian model to explain the origin of the long-lived coherence in pigment-protein complexes. We show that the memory effect of the discrete vibrational modes produces a long oscillating tail in the coherence. We further use the recently proposed measure to quantify the non-Markovianity of the system and find out the prolonged coherence is highly correlated to it.

DOI: 10.1103/PhysRevE.89.042147 PACS number(s): 05.40.−a, 03.65.Yz, 31.70.Hq

I. INTRODUCTION

The phenomenon of excitation energy transfer (EET) is widely observed in photosynthetic pigment-protein complexes (PPCs), such as the Fenna-Matthews-Olson (FMO) antenna complex and the light-harvesting II (LH2) complex [1]. Many theoretical works based on the diffusion-rate equations with the Markovian approximation have been proposed [2–4]. In these studies, one usually employs the assumption of the weak system-environment coupling (or the ultrashort environmental correlation time), such that the environment only leads to the Markovian damping [5]. In real experiments, however, the time scales of the excitation dynamics, phonon field reorganization, and the system-environment interaction are comparable [6,7]. Therefore, the actual dynamics should go beyond the weak-coupling regime.

Recently, the long-lasting beating signals have been reported in the experiments on PPCs by using the two-dimensional photon echo technique [8–10]. This provides a strong evidence for both the wave-like behavior of the EET phenomenon in chromophoric molecules network and the existence of the persistent quantum coherence. In the past few years, the phenomena have been discussed extensively [11–13]. However, there are still many open questions associated with the presence of robust quantum coherence against the surrounding environment. For example, its impact on the efficiency of the EET [14,15], the role played by the surrounding environments [16], and the non-Markovian memory effect. In order to construct a proper model that can reproduce useful insights, many methods, such as non-Markovian second-order perturbation theory [17], the polaron transformation [18–21], and the hierarchy approaches [17,22–25], have been used to catch the underlying mechanisms.

To explore the correlation between the long-lived coherence and the non-Markovian memory effect, we present here an analytical theory for a system coupled to the environments containing both the locally continuous and the discrete vibrational modes (commonly shared by several pigments) [26–28]. As a main result, we find that the memory effect of the discrete vibrational modes produces a long oscillating tail and the coherence time is significantly prolonged. To address its relation to the non-Markovian effect, we use the recently developed measure [29] to quantify the non-Markovianity of the system. By observing the results at different coupling strength and temperatures, we find that the higher non-Markovianity corresponds to the stronger oscillating tail and may explain the long-lived coherence (or the rephasing mechanism [16]) up to picosecond.

II. THEORY

A. Model

Considering that the pigment aggregation consists of N pigments. In the single-excitation manifold, the system Hamiltonian $\widehat{H}_{\rm sys}$, is written as

$$\widehat{H}_{\rm sys} = \sum_{j=1}^{N} \hbar\omega_j |j\rangle\langle j| + \sum_{j<k} J_{j,k}(|j\rangle\langle k| + |k\rangle\langle j|), \quad (1)$$

where $\hbar\omega_j$ is the energy of the jth site (pigment) and $J_{j,k}$ is the electronic coupling between the jth and kth sites. The number of pigments in an aggregation varies in different species, ranging from 6 in the reaction center (RC) [30–32], 7 in the FMO [33,34], to 8 and 16 in the B800 and B850 BChl ring of the LH2 [35,36], respectively. Normally, they are very closely packed by groups of long protein subunit helices. For example, the molecules of the RC in photosystem II from *Thermosynechococcus elongatus* is enclosed by D1 and D2 subunit with average nearest-neighbor distance about 10 Å [32].

In addition to the short intermolecular distance, it has been suggested that highly correlated environment is responsible for the long-lived coherence [8]. Thus, it is plausible to assume that the pigments share some *discrete and common* vibrational modes in their vicinity

$$\widehat{H}_{\rm sys-vib} = \sum_{j=1}^{N} \sum_{\mathbf{k}} |j\rangle\langle j| \otimes (\hbar g_{j,\mathbf{k}} \hat{b}_{\mathbf{k}}^{\dagger} + \hbar g_{j,\mathbf{k}}^{*} \hat{b}_{\mathbf{k}}), \quad (2)$$

where $g_{j,\mathbf{k}}$ is the coupling strength and $\hat{b}_{\mathbf{k}}$ ($\hat{b}_{\mathbf{k}}^{\dagger}$) is the annihilation (creation) operator describing the *discrete and common* vibrational modes. From now on, the *discrete and common* vibrational modes will be rephrased as the *common modes* for simplicity. Besides the coupling to the common

*yuehnan@mail.ncku.edu.tw

modes, we also assume that each pigment is coupled to its individual local environment

$$\widehat{H}_{\text{sys-env}} = \sum_{j=1}^{N} \sum_{\mathbf{q}} |j\rangle\langle j| \otimes (\hbar g_{j,\mathbf{q}} \hat{a}^{\dagger}_{j,\mathbf{q}} + \hbar g^{*}_{j,\mathbf{q}} \hat{a}_{j,\mathbf{q}}), \quad (3)$$

where $g_{j,\mathbf{q}}$ is the local coupling strength of the jth site and $\hat{a}_{j,\mathbf{q}}$ ($\hat{a}^{\dagger}_{j,\mathbf{q}}$) is the annihilation (creation) operator of the jth local environmental modes.

The total Hamiltonian describing the photosynthetic EET processes is then written as

$$\widehat{H}_T = \widehat{H}_{\text{sys}} + \widehat{H}_{\text{vib}} + \widehat{H}_{\text{sys-vib}} + \widehat{H}_{\text{env}} + \widehat{H}_{\text{sys-env}}, \quad (4)$$

where

$$\widehat{H}_{\text{vib}} = \sum_{\mathbf{k}} \hbar\omega_{\mathbf{k}} \hat{b}^{\dagger}_{\mathbf{k}} \hat{b}_{\mathbf{k}} \quad (5)$$

and

$$\widehat{H}_{\text{env}} = \sum_{j=1}^{N} \sum_{\mathbf{q}} \hbar\omega_{j,\mathbf{q}} \hat{a}^{\dagger}_{j,\mathbf{q}} \hat{a}_{j,\mathbf{q}}. \quad (6)$$

B. Polaron transformation

In the EET phenomenon, the electronic coupling plays an important role in facilitating energy transfer between chromophores. Several approaches have been developed for different coupling regimes. In the weak electronic-coupling regime, the Förster theory leads to the diffusion-rate equations. On the other hand, in the strong electronic-coupling regime, the Redfield theory considers the dynamics of the delocalized states dissipated by the weak environmental perturbation. However, none of the conventional Markovian treatments can adequately describe the EET process in the intermediate coupling regime due to the comparable scale of the electronic coupling, phonon field reorganization, and the system-environment interaction. [6,37]. Although numerically nonperturbative approaches have been successfully applied to provide the insights of the dynamics [38], one usually requires special numerical implementations to perform the intensive numerical calculations [16]. To gain the physical insights straightforwardly, we adopt here the small-polaron quantum master equation, which has been successfully applied to describe the EET processes in the intermediate coupling regime [18,19,39].

The first step is to perform the unitary polaron transformation with respect to the common modes $\hat{b}_{\mathbf{k}}$: $\widetilde{H} = e^{\widehat{S}} \widehat{H} e^{-\widehat{S}}$, where $\widehat{S} = \sum_{j=1}^{N} \sum_{\mathbf{k}} |j\rangle\langle j| \otimes (\frac{g_{j,\mathbf{k}}}{\omega_{\mathbf{k}}} \hat{b}^{\dagger}_{\mathbf{k}} - \frac{g^{*}_{j,\mathbf{k}}}{\omega_{\mathbf{k}}} \hat{b}_{\mathbf{k}})$. The transformed total Hamiltonian can be rearranged as

$$\widetilde{H}_T = \widetilde{H}_{\text{sys}} + \widehat{H}_{\text{vib}} + \widetilde{H}_{\text{fluc}} + \widehat{H}_{\text{env}} + \widehat{H}_{\text{sys-env}}, \quad (7)$$

where

$$\widetilde{H}_{\text{sys}} = \sum_{j=1}^{N} \left(\hbar\omega_j - \hbar \sum_{\mathbf{k}} \frac{|g_{j,\mathbf{k}}|^2}{\omega_{\mathbf{k}}} \right) |j\rangle\langle j| + \sum_{j<k} (J_{j,k} B_{j,k} |j\rangle\langle k| + J_{k,j} B_{k,j} |k\rangle\langle j|), \quad (8)$$

and

$$\widetilde{H}_{\text{fluc}} = \sum_{j<k} [J_{j,k} |j\rangle\langle k| \otimes (\widehat{D}_j \widehat{D}^{\dagger}_k - B_{j,k}) + J_{k,j} |k\rangle\langle j| \otimes (\widehat{D}_k \widehat{D}^{\dagger}_j - B_{k,j})]. \quad (9)$$

Here, the expectation value $B_{j,k} = \langle \widehat{D}_j \widehat{D}^{\dagger}_k \rangle$ and $\widehat{D}_j = \exp[\sum_{\mathbf{k}} (\frac{g_{j,\mathbf{k}}}{\omega_{\mathbf{k}}} \hat{b}^{\dagger}_{\mathbf{k}} - \frac{g^{*}_{j,\mathbf{k}}}{\omega_{\mathbf{k}}} \hat{b}_{\mathbf{k}})]$ is the displacement operator. Note that $\widetilde{H}_{\text{fluc}}$ can be considered as the fluctuation of the transformed electronic coupling from its average value.

C. Master equation

In the interaction picture, the time evolution of the total density matrix is governed by the following equation of motion:

$$\frac{\partial}{\partial t} \rho_{\text{tot}}(t) = -\frac{i}{\hbar} [\widetilde{H}_{\text{fluc}}(t), \rho_{\text{tot}}(t)] - \frac{i}{\hbar} [\widehat{H}_{\text{sys-env}}(t), \rho_{\text{tot}}(t)]. \quad (10)$$

In our model, the non-Markovian effect will be taken into account by the time integral over the past history of $\widetilde{H}_{\text{fluc}}(t)$. However, in contrast to the non-Markovian interaction $\widetilde{H}_{\text{fluc}}(t)$ from the common modes, the PPCs are immersed in a humid physiological environment or embedded in a huge protein matrix [40–42]. The interaction with such environment is described by $\widehat{H}_{\text{sys-env}}$ and can be treated Markovianly in the Redfield limit, namely, with small reorganization energy [6,17,22]. The master equation is then written as

$$\frac{\partial}{\partial t} \rho_{\text{sys}}(t) = -\frac{i}{\hbar} \text{Tr}_{\text{vib}} [\widetilde{H}_{\text{fluc}}(t), \rho_{\text{sys}}(t) \otimes \rho_{\text{vib}}] - \frac{1}{\hbar^2} \text{Tr}_{\text{env}} \times \int_0^{\infty} [\widehat{H}_{\text{sys-env}}(t), [\widehat{H}_{\text{sys-env}}(t-\tau), \rho_{\text{sys}}(t) \otimes \rho_{\text{env}}]] d\tau, \quad (11)$$

where ρ_{vib} and ρ_{env} are the density matrices of the common modes and the local environment, respectively. Express the master equation in the *exciton* basis $\{|\mu\rangle\}$, i.e., the eigenbasis of $\widetilde{H}_{\text{sys}}$ with $\widetilde{H}_{\text{sys}} |\mu\rangle = \hbar\omega_{\mu} |\mu\rangle$. The master equation becomes

$$\begin{aligned} \frac{\partial}{\partial t} \rho_{\text{sys}}(t) &= -\frac{i}{\hbar} \text{Tr}_{\text{vib}} [\widetilde{H}_{\text{fluc}}(t), \rho_{\text{sys}}(t) \otimes \rho_{\text{vib}}] \\ &+ \sum_{j,\mu,\nu,\mu',\nu'} \int_0^{\infty} \{ G_j(\tau) e^{i\omega_{\nu',\mu'}\tau} A_{j,\mu,\nu} A_{j,\mu',\nu'} e^{i\omega_{\mu,\nu}t} e^{i\omega_{\mu',\nu'}t} \\ &\times [\hat{\sigma}_{\mu',\nu'} \rho_{\text{sys}}(t) \hat{\sigma}_{\mu,\nu} - \hat{\sigma}_{\mu,\nu} \hat{\sigma}_{\mu',\nu'} \rho_{\text{sys}}(t)] \} d\tau \\ &+ \sum_{j,\mu,\nu,\mu',\nu'} \int_0^{\infty} \{ G^{*}_j(\tau) e^{-i\omega_{\nu',\mu'}\tau} A_{j,\nu,\mu} A_{j,\nu',\mu'} e^{-i\omega_{\mu,\nu}t} \\ &\times e^{-i\omega_{\mu',\nu'}t} [\hat{\sigma}_{\nu,\mu} \rho_{\text{sys}}(t) \hat{\sigma}_{\nu',\mu'} - \rho_{\text{sys}}(t) \hat{\sigma}_{\nu',\mu'} \hat{\sigma}_{\nu,\mu}] \} d\tau , \end{aligned} \quad (12)$$

where $A_{j,\mu,\nu} = \langle \mu | j \rangle \langle j | \nu \rangle$, $\hat{\sigma}_{\mu,\nu} = |\mu\rangle\langle\nu|$, $\omega_{\mu,\nu} = \omega_{\mu} - \omega_{\nu}$, and $G_j(\tau) = \int_0^{\infty} J_j(\omega) [\cos\omega\tau \coth(\frac{\hbar\omega}{2k_B T}) - i \sin\omega\tau] d\omega$ is

the correlation function with the spectral density function defined as $J_j(\omega) = \sum_{\mathbf{q}} |g_{j,\mathbf{q}}|^2 \delta(\omega - \omega_{j,\mathbf{q}})$.

By applying the secular approximation, all frequency mismatching terms in Eq. (12) with $\omega_{\nu,\mu} \neq -\omega_{\nu',\mu'}$ are neglected. If one further assumes $\int_0^\infty G_j(\tau) e^{i\omega_{\mu,\nu}\tau} d\tau \approx \frac{1}{2}\gamma_{j,\mu,\nu} - iS_{j,\mu,\nu}$, the master equation can be simplified

$$\frac{\partial}{\partial t}\rho_{\rm sys}(t) = -\frac{i}{\hbar}{\rm Tr}_{\rm vib}[\widetilde{H}_{\rm fluc}(t), \rho_{\rm sys}(t)\otimes\rho_{\rm vib}] - \frac{i}{\hbar}[\widehat{H}_{\rm reg}, \rho_{\rm sys}(t)] + \Re\{\rho_{\rm sys}(t)\}, \quad (13)$$

where $\widehat{H}_{\rm reg} = \sum_{j,\mu,\nu} -\hbar S_{j,\mu,\nu}|A_{j,\mu,\nu}|^2 |\mu\rangle\langle\mu|$ is the reorganization energy induced by the local environment and the Markovian dissipator takes the form

$$\begin{aligned}\Re\{\rho_{\rm sys}(t)\} = &\sum_{j,\mu,\mu'} \gamma_{j,\mu',\mu'} A_{j,\mu,\mu} A_{j,\mu',\mu'} \\ &\times \left\{\hat{\sigma}_{\mu,\mu}\rho_{\rm sys}(t)\hat{\sigma}_{\mu',\mu'} - \frac{1}{2}[\hat{\sigma}_{\mu',\mu'}\hat{\sigma}_{\mu,\mu}, \rho_{sys}(t)]\right\} \\ &+ \sum_{j,\mu\neq\nu} \gamma_{j,\mu,\nu}|A_{j,\mu,\nu}|^2 \\ &\times \left\{\hat{\sigma}_{\nu,\mu}\rho_{\rm sys}(t)\hat{\sigma}_{\mu,\nu} - \frac{1}{2}[\hat{\sigma}_{\mu,\nu}\hat{\sigma}_{\nu,\mu}, \rho_{\rm sys}(t)]\right\}. \end{aligned} \quad (14)$$

The first term on the right-hand side of Eq. (14) gives the bath-induced pure dephasing channel in the exciton basis, while the second term gives the exciton migration.

Let us rewrite the master equation in the site basis, which is appropriate for considering the EET phenomenon between the pigments. Although $\widetilde{H}_{\rm sys}$ and $\widehat{H}_{\rm reg}$ are diagonal in the exciton basis $\{|\mu\rangle\}$, it is not the case in the site basis due to the electronic coupling between each site. Hence, we can regroup them into the diagonal part and off-diagonal part:

$$\widetilde{H}_{\rm sys} + \widehat{H}_{\rm reg} = \widehat{H}_0 + \widehat{H}_{\rm ele}, \quad (15)$$

where $\widehat{H}_0 = \sum_{j=1}^N \hbar\omega'_j |j\rangle\langle j|$ is the diagonal part corresponding to the site energy containing the modulation given by $\widehat{H}_{\rm reg}$ with

$$\omega'_j = \hbar\omega_j - \hbar\sum_{\mathbf{k}} \frac{|g_{j,\mathbf{k}}|^2}{\omega_{\mathbf{k}}} - \sum_{k,\mu,\nu} \hbar S_{k,\mu,\nu}|A_{k,\mu,\nu}|^2 A_{j,\mu,\mu}, \quad (16)$$

and $\widehat{H}_{\rm ele} = \sum_{j<k}(J'_{j,k}B_{j,k}|j\rangle\langle k| + J'_{k,j}B_{k,j}|k\rangle\langle j|)$ is the off-diagonal part corresponding to the electronic coupling between each site modulated by $\widehat{H}_{\rm reg}$ with

$$J'_{j,k} = J_{j,k} - \sum_{l,\mu,\nu} \hbar\frac{S_{l,\mu,\nu}}{B_{j,k}}|A_{l,\mu,\nu}|^2(\langle j|\mu\rangle\langle\mu|k\rangle). \quad (17)$$

D. Non-Markovian treatment to the common modes

It has been pointed out that the discrete vibrational modes may be responsible for the long-lived coherence [16,26,28]. However, in Ref. [16], the discrete vibrational modes coupled to each site is noncorrelated and a special numerical implementation is employed in their simulation. Thus, to gain an analytic theory, we apply the second-order time convolution method to the interaction between the pigments and the common modes, $\widetilde{H}_{\rm fluc}$, and obtain the following master equation:

$$\begin{aligned}\frac{\partial}{\partial t}&\rho_{\rm sys}(t) \\ &= -\frac{i}{\hbar}[\widehat{H}_{\rm ele}(t), \rho_{\rm sys}(t)] + \Re\{\rho_{\rm sys}(t)\} - \frac{1}{\hbar^2}Tr_{\rm vib} \\ &\quad\times\int_0^t [\widetilde{H}_{\rm fluc}(t), [\widetilde{H}_{\rm fluc}(\tau), \rho_{\rm sys}(\tau)\otimes\rho_{\rm vib}]]d\tau. \end{aligned} \quad (18)$$

Explicitly expanding Eq. (18) in the site basis leads to a set of coupled integrodifferential equations of the density matrix elements $\{\rho_{j,k}(t)\}$

$$\begin{aligned}\frac{\partial}{\partial t}&e^{-i\omega'_{j,k}t}\rho_{j,k}(t) \\ &= -i\omega'_{j,k}e^{-i\omega'_{j,k}t}\rho_{j,k}(t) + \sum_{j',k'}\Re_{j,k,j',k'}e^{-i\omega_{j',k'}t}\rho_{j',k'}(t) \\ &\quad - \frac{i}{\hbar}\sum_{l\neq j} J'_{j,l}B_{j,l}e^{-i\omega'_{l,k}t}\rho_{l,k}(t) + \frac{i}{\hbar}\sum_{l\neq k} J'_{l,k}B_{l,k}e^{-i\omega'_{j,l}t}\rho_{j,l}(t) \\ &\quad + \frac{1}{\hbar^2}\sum_{l,m}\int_0^t f_{l,m}(t-\tau)e^{-i\omega'_{l,m}\tau}\rho_{l,m}(\tau)d\tau. \end{aligned} \quad (19)$$

One can notice that the memory effects are taken into account in terms of the convolution of the memory kernel $f_{l,m}(t)$. Its detailed expression is given in the Appendix. One approach to solve the coupled integrodifferential Eq. (19) is to invoke the Laplace transformation. After carefully analyzing properties of the poles, one can find out that each pole is of the first order with a negative real part. The standard contour integration then can be applied to accomplish the inverse Laplace transformation.

III. RESULTS AND DISCUSSIONS

A. The dimer model

We now apply our theory to a dimer model consisting of two sites denoted by $|L\rangle$ and $|R\rangle$, as illustrated in Fig. 1. The dimer parameters used in the calculations are $\omega_L - \omega_R = 100\,{\rm cm}^{-1}$ and $J_{L,R} = 100\,{\rm cm}^{-1}$. The energy difference of two exciton eigenstates $|e_1\rangle$, $|e_2\rangle$ is $\omega_{1,2} = 200\,{\rm cm}^{-1}$. For simplicity, only

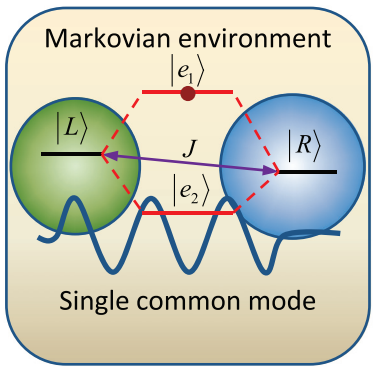

FIG. 1. (Color online) Schematic illustration of the dimer model. The two sites are denoted by $|L\rangle$ and $|R\rangle$. They couple to each other via an electronic coupling J and form two delocalized eigenstates $|e_1\rangle$, $|e_2\rangle$. The two sites share a single common mode, and each site has its own local environment, which is treated Markovianly.

single common mode with $\omega_{\mathbf{k}} = 150\,\mathrm{cm}^{-1}$, $g_{L,\mathbf{k}} = 75\,\mathrm{cm}^{-1}$, and $g_{R,\mathbf{k}} = 60\,\mathrm{cm}^{-1}$ is considered for the non-Markovian effect.

Each local environment is assumed to be homogeneous, such that the spectral density of each site is the same. The information of the spectral density can be extracted from the hole-burning [43] or fluorescence line-narrowing (FLN) spectra [26–28]. The over-damped Brownian oscillation model has been found to fit the experimental data well [44] and is widely used in many theoretical works [21,24]:

$$J_j(\omega) = J(\omega) = \frac{2\lambda\gamma}{\pi}\frac{\omega}{\omega^2+\gamma^2}. \tag{20}$$

According to Refs. [17,22], to ensure the accuracy of Markovian treatment on the local environment, λ should be less than electronic coupling $J_{L,R}$ such that it can approach the Redfield limit. Hence the following values are chosen: $\lambda = 20\,\mathrm{cm}^{-1}$ and $\gamma = 50\,\mathrm{cm}^{-1}(\gamma^{-1} = 106\,\mathrm{fs})$, which is shown to give the results that coincide with the experimental observations [17].

To explicitly show the long-lived coherence by the common mode, we compare the results of our non-Markovian dimer model with those of a Markovian counterpart without the common mode. Figure 2 shows the time evolutions of the populations of the L site and R site at different temperatures for both the non-Markovian (solid curves) and Markovian (dashed curves) models. As seen, the oscillating amplitudes of both models are suppressed when increasing the temperature. In addition, the non-Markovian model gives the longer oscillating amplitudes in time than those of the Markovian model.

In many recent photon echo experiments, the coherence in the exciton basis was demonstrated. In Fig. 3(a), we show the time evolutions of the coherence in the exciton basis for both models with an initial state $\rho_{\mathrm{sys}}(0) = |L\rangle\langle L|$; i.e., the absorbed photon energy is transmitted from the antenna pigments into the L site of the dimer. In the absence of the common mode, the coherence in the Markovian model (dashed curves) decays monotonically to zero within 400 to 600 fs. In contrast, the non-Markovian model (solid curves) provides prominent oscillations and sustains much longer coherence time. Besides, one also notes that the profile in the non-Markovian model consists of two components: One is a fast monotonic decay by the outer environment roughly on the same time scale as Markovian counterpart, and the other is a multifrequency beating pattern induced by the non-Markovian interaction with the common mode. Moreover, when the time goes beyond 500 fs, the coherence of the Markovian model almost dies out in the exciton basis. However, in the non-Markovian model, the coherence is provided (or generated) by the common mode and can last a long time.

To further confirm that the beating tail in the non-Markovian model is exactly from the interaction with the common mode, in Fig. 3(b), we show the coherence in the exciton basis with the initial state $\rho_{\mathrm{sys}}(0) = |e_1\rangle\langle e_1|$. No initial coherence in the exciton basis is present for such an initial condition and hence no coherence is present in the Markovian model (dashed curves). However, in the non-Markovian model (solid curves), coherence can be induced by the common mode even without the initial coherence. This phenomenon is similar to the Rabi-oscillation in quantum optics and has also been observed by Chin *et al.* [16]. We stress that the underlying physics is from the non-Markovian coupling to the common mode.

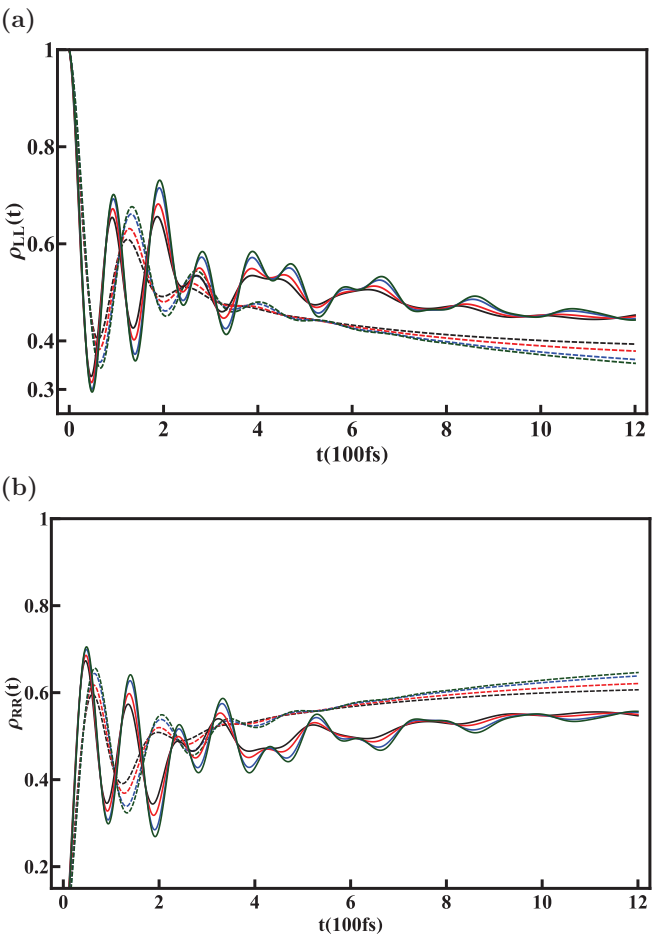

FIG. 2. (Color online) The populations of (a) the L site and (b) the R site with temperature at 180 K (green), 200 K (blue), 250 K (red), and 300 K (black) for both the Markovian (dashed) and non-Markovian (solid) models. Long oscillating tails are induced by the single common mode and are suppressed when increasing the temperature.

B. Degree of the non-Markovianity

To assert on the relation between the non-Markovian effect and long-lived coherence, we proceed to study the measure of the non-Markovianity. Recently, many efforts have been devoted to construct a proper measure of the non-Markovianity. At least two different approaches have been proposed. One approach is proposed by Breuer *et al.* [45]. The non-Markovianity is defined by monitoring the temporal backflow of the information from the environment into the system. Another approach is based on the idea of the divisibility of a quantum process applied to a quantum system [46,47]. This concept is used by Rivas *et al.* [29] to construct a different measure of the non-Markovianity. In the following, we will adopt the measure proposed by Rivas *et al.* [29] and introduce an ancillary dimer in order to calculate the non-Markovianity.

Suppose that $\mathcal{A}^d$ is a $C^\star$-algebra of linear operator on the d-dimensional Hilbert space $\mathcal{H}^d$. A trace-preserving map $\mathcal{E}(t,0) : \mathcal{A}^d \to \mathcal{A}^d$ mapping an initial state $\rho(0)$ to a final state $\rho(t)$ is said to be completely positive (CP) if $\mathbf{I}^n \otimes \mathcal{E} : \mathcal{A}^{n+d} \to \mathcal{A}^{n+d}$ is also positive for any nonnegative integer n, where $\mathbf{I}^n$ is an identity operation on $\mathcal{A}^n$. Every authentic quantum process

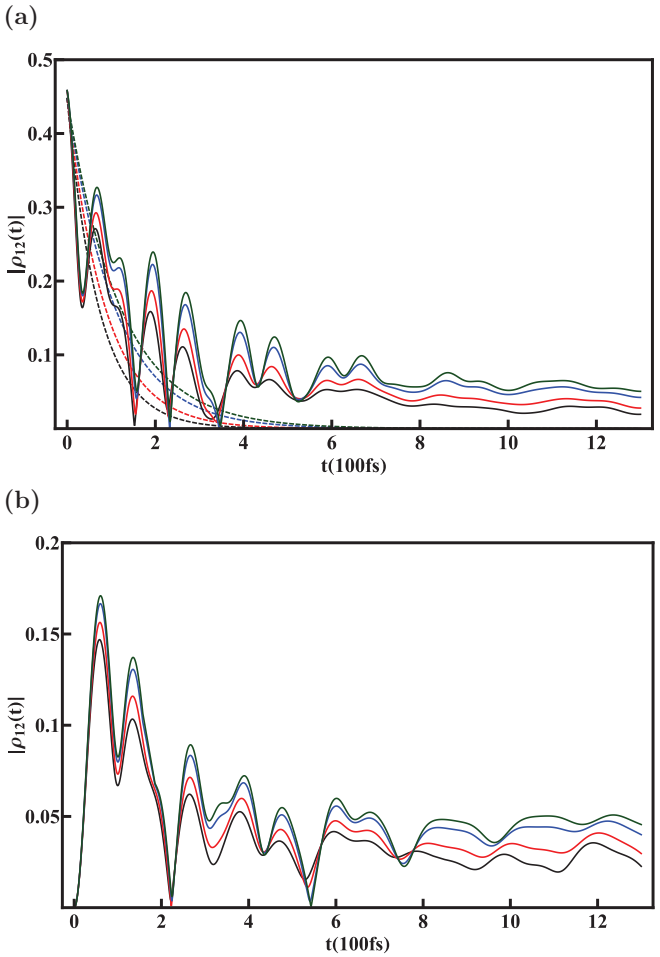

FIG. 3. (Color online) Time evolutions of the coherence between the two exciton basis with temperature at 180 K (green), 200 K (blue), 250 K (red), and 300 K (black) for both the Markovian (dashed) and non-Markovian (solid) models. (a) The initial condition, $\rho_{\rm sys}(0) = |L\rangle\langle L|$, is used and the non-Markovian profiles show two components as explained in the context, whereas the Markovian ones are merely monotonic decay. (b) The initial condition, $\rho_{\rm sys}(0) = |e_1\rangle\langle e_1|$, is used and the oscillating tails can still be induced by the single common mode, whereas no coherence is present in the Markovian model.

should be CP to ensure that we can measure a legal quantum state ρ. Let us define the trace norm $\|\cdot\|_1$ of a matrix A as

$$\|A\|_1 = \mathrm{Tr}\sqrt{A^\dagger A}\,. \tag{21}$$

A CP quantum process $\mathcal{E}(t+\tau,0)$ is said to be divisible if, for any t ($\tau > 0$), one can find another CP process $\Lambda(t+\tau,t)$ such that

$$\mathcal{E}(t+\tau,0) = \Lambda(t+\tau,t)\circ\mathcal{E}(t,0). \tag{22}$$

A process $\mathcal{E}$ is said to be Markovian if it is divisible. Hence, the measure of the non-Markovianity proposed by Rivas *et al.* [29] is the degree of a process deviating from being divisible

$$g(t) = \lim_{\epsilon\to 0^+}\frac{\|(\mathbf{I}^d\otimes\Lambda(t+\epsilon,t))(|\Psi\rangle\langle\Psi|)\|_1 - 1}{\epsilon}\,, \tag{23}$$

where $|\Psi\rangle$ denotes a maximally entangled state in $\mathcal{H}^d\otimes\mathcal{H}^d$. Due to the Choi-Jamiołkowski isomorphism [48,49],

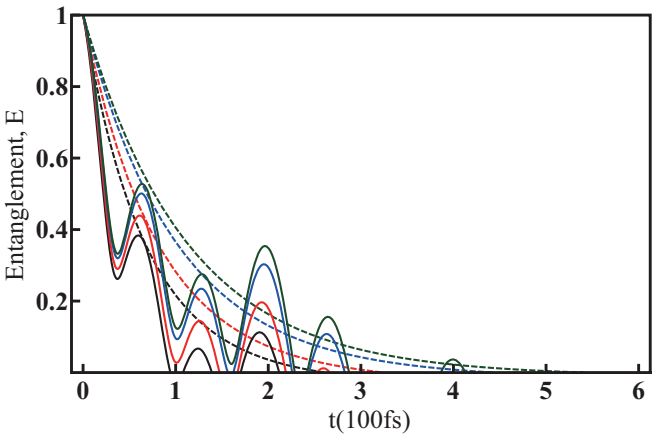

FIG. 4. (Color online) The entanglement between a dimer system and its corresponding ancillary dimer with temperature at 180 K (green), 200 K (blue), 250 K (red), and 300 K (black) for both the Markovian (dashed) and non-Markovian (solid) models.

$g(t)\geqslant 0, \forall t > 0$, and $g(t) = 0$ if and only if $\Lambda(t+\epsilon,t)$ is CP, namely, $\mathcal{E}$ is divisible and Markovian.

However, from the practical point of view, Eq. (23) is not necessarily useful in some situations. For example, if the detailed information of the system cannot exactly be extracted from the experimental data, $\mathcal{E}(t,0)$ cannot be properly constructed. Hence, a replacement of Eq. (23) is suggested: Every local CP operation can never increase the entanglement $\mathbf{E}$ between a system and another copy of an ancillary system,

$$\mathbf{E}(\rho_{\rm sys,anc}) \geqslant \mathbf{E}[(\mathcal{E}_{\rm sys}\otimes\mathcal{E}_{\rm anc})(\rho_{\rm sys,anc})]. \tag{24}$$

Consequently, the degree of the non-Markovianity within a given time interval $[0,t]$ can be estimated [29] by

$$\mathcal{I} = \int_0^t \left|\frac{d}{d\tau}\mathbf{E}\{[\mathbf{I}^d\otimes\mathcal{E}(\tau,0)](|\Psi\rangle\langle\Psi|)\}\right| d\tau - \Delta\mathbf{E}_t, \tag{25}$$

where $\Delta\mathbf{E}_t = \mathbf{E}(|\Psi\rangle\langle\Psi|) - \mathbf{E}\{[\mathbf{I}^d\otimes\mathcal{E}(t,0)](|\Psi\rangle\langle\Psi|)\}$. Given a Markovian process $\mathcal{E}$, the quantity $\mathbf{E}\{[\mathbf{I}^d\otimes\mathcal{E}(\tau,0)](|\Psi\rangle\langle\Psi|)\}$ is monotonically decreasing function in time.

In Fig. 4, we calculate the entanglement between our non-Markovian dimer model and a copy of well-isolated ancillary dimer. The measure of the entanglement is defined by the concurrence [50]. For comparison, we also plot the Markovian counterpart (dashed curves). The wavy solid curves are good indications of the non-Markovianity. As seen, the long wavy tails sink earlier at the higher temperatures, i.e., the non-Markovianity decreases when increasing the temperature. Without the common mode, the monotonically decreasing dashed lines illustrate that the dimer system undergoes a Markovian process and the environment continuously destroys the entanglement between the dimer system and its corresponding ancillary dimer.

In Fig. 5(a), we plot the dependence of the non-Markovianity (due to the common mode) on temperature at different coupling strength $g_{L,R}$. The parameters for the blue dots are the same as those in previous figures. For the black dots, we choose $g_L = 165\,\mathrm{cm}^{-1}$, $g_R = 135\,\mathrm{cm}^{-1}$, and for the red dots, $g_L = 157.5\,\mathrm{cm}^{-1}$, $g_R = 142.5\,\mathrm{cm}^{-1}$ are used. It clearly shows that a larger coupling strength or a larger difference in $g_{L,R}$ will produce a stronger non-Markovianity.

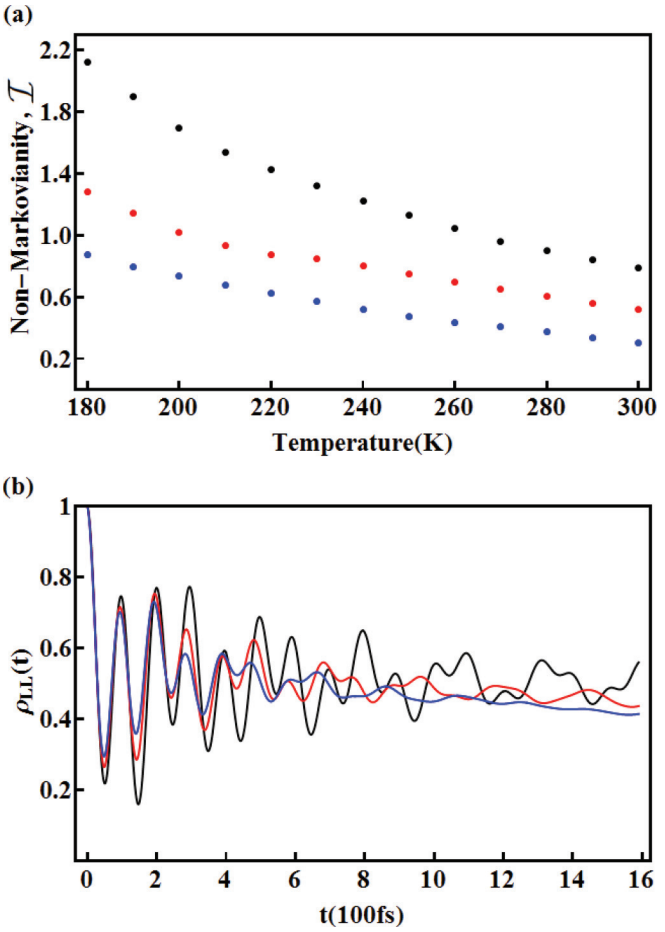

FIG. 5. (Color online) (a) Non-Markovianity versus temperature for different couplings to the common mode. The parameters for the blue dots are the same as those described in the legends of the previous figures. Black and red dots are obtained by using the stronger couplings of $g_{L,\mathbf{k}}$ and $g_{R,\mathbf{k}}$, as illustrated in the main text. A stronger coupling to the common mode can induce a larger non-Markovianity $\mathcal{I}$. (b) Time evolutions of the populations at $T = 180$ K. A stronger coupling to the common mode generates the longer and larger oscillating behavior.

Meanwhile, the non-Markovianity decreases when increasing the temperature, as expected in Fig. 4.

To further show the connection of the long-lived coherence to the non-Markovianity, in Fig. 5(b), we plot the populations of the three different values of coupling strength at 180 K. In Fig. 5(a), the degrees of the non-Markovianity for the black, red, and blue dots at 180 K take the values $\mathcal{I} = 2.12$, 1.23, and 0.87, respectively, and their corresponding dynamics are depicted in Fig. 5(b) with the same colors. It can be seen that the black curve persists the obvious oscillations longer than 1.6 ps. The red curve also has a long oscillating tail, but its amplitude is much smaller than the black one. The oscillations in the blue curve almost die out after 1.2 ps. Hence, we can conclude that a stronger coupling to the common mode induces the larger non-Markovianity and can support longer, energetic EET process.

IV. CONCLUSION

In conclusion, we propose an analytical non-Markovian model to gain the physical insights of the long-lived coherence straightforwardly without invoking any specific numerical implementation. Our theory suggests that the common modes play a crucial role in EET process. With the presence of the common modes, the absorbed photon energy can persist hopping for much longer time and hence the EET becomes more energetic even at physiological temperature. This provides an approach to study the environmentally enhanced EET efficiency.

In addition, the non-Markovian profiles consist of two components: a monotonic decay and a multifrequency beating, whereas the Markovian model can only decay monotonically. The coherence can be induced by the common modes even without the initial coherence in the exciton basis. These phenomena suggest that the common modes may induce the coherence and can be analogous to an externally driven Rabi-oscillation in quantum optics.

To address the relation between these effects and the non-Markovianity, a measurement in Ref. [29] is applied to our model. One can find out that a stronger coupling to the common modes can produce a larger non-Markovianity and generate a longer and larger oscillating amplitude. These confirm the connections between the common modes, the non-Markovianity, and the long-lived coherence.

ACKNOWLEDGMENTS

The authors thank Y. C. Cheng and A. Buchleitner for helpful comments. This work is supported partially by the National Center for Theoretical Sciences and National Science Council, Taiwan, Grant No. NSC 101-2628-M-006-003-MY3.

APPENDIX: DETAILED EXPRESSION OF MEMORY KERNEL

The detailed expression of the integral term of Eq. (19) is given by $\forall j,k$,

$$\begin{aligned}\sum_{l,m}\int_0^t f_{l,m}(t-\tau)e^{-i\omega'_{l,m}\tau}\rho_{l,m}(\tau)d\tau = &\sum_{l\neq j,m\neq k}\int_0^t J_{j,l}J_{m,k}e^{i\omega'_{k,l}(t-\tau)}[\langle\widehat{D}_m(\tau)\widehat{D}_k^\dagger(\tau)\widehat{D}_j(t)\widehat{D}_l^\dagger(t)\rangle - B_{j,l}B_{m,k}]e^{-i\omega'_{l,m}\tau}\rho_{l,m}(\tau)d\tau\\ &-\sum_{l\neq j,m\neq l}\int_0^t J_{j,l}J_{l,m}e^{i\omega'_{k,l}(t-\tau)}[\langle\widehat{D}_j(t)\widehat{D}_l^\dagger(t)\widehat{D}_l(\tau)\widehat{D}_m^\dagger(\tau)\rangle - B_{j,l}B_{l,m}]e^{-i\omega'_{m,k}\tau}\rho_{m,k}(\tau)d\tau\\ &+\sum_{l\neq j,m\neq k}\int_0^t J_{m,k}J_{j,l}e^{i\omega'_{m,j}(t-\tau)}[\langle\widehat{D}_m(t)\widehat{D}_k^\dagger(t)\widehat{D}_j(\tau)\widehat{D}_l^\dagger(\tau)\rangle - B_{m,k}B_{j,l}]e^{-i\omega'_{l,m}\tau}\rho_{l,m}(\tau)d\tau\\ &-\sum_{l\neq m,m\neq k}\int_0^t J_{m,k}J_{l,m}e^{i\omega'_{m,j}(t-\tau)}[\langle\widehat{D}_l(\tau)\widehat{D}_m^\dagger(\tau)\widehat{D}_m(t)\widehat{D}_k^\dagger(t)\rangle - B_{l,m}B_{m,k}]e^{-i\omega'_{j,l}\tau}\rho_{j,l}(\tau)d\tau.\end{aligned} \tag{A1}$$

[1] R. K. Chain and D. I. Arnon, Proc. Natl. Acad. Sci. USA **74**, 3377 (1977).
[2] W. M. Zhang, T. Meier, V. Chernyak, and S. Mukamel, J. Chem. Phys. **108**, 7763 (1998).
[3] M. Yang and G. R. Fleming, Chem. Phys. **275**, 355 (2002).
[4] J. Adolphs and T. Renger, Biophys. J. **91**, 2778 (2006).
[5] H. P. Breuer and F. Petruccione, *The Theory of Open Quantum Systems* (Oxford University Press, New York, 2002).
[6] A. Ishizaki and G. R. Fleming, J. Chem. Phys. **130**, 234110 (2009).
[7] P. Huo and D. F. Coker, J. Chem. Phys. **133**, 184108 (2010).
[8] H. Lee, Y.-C. Cheng, and G. R. Fleming, Science **316**, 1462 (2007).
[9] G. S. Engel, T. R. Calhoun, E. L. Read, T.-K. Ahn, T. Mančal, Y.-C. Cheng, R. E. Blankenship, and G. R. Fleming, Nature **446**, 782 (2007).
[10] G. Panitchayangkoon, D. Hayes, K. A. Fransted, J. R. Caram, E. Harel, J. Wen, R. E. Blankenship, and G. S. Engel, Proc. Natl. Acad. Sci. USA **107**, 12766 (2010).
[11] Y.-C. Cheng and G. R. Fleming, Annu. Rev. Phys. Chem. **60**, 241 (2009).
[12] N. Lambert, Y.-N. Chen, Y.-C. Cheng, C.-M. Li, G.-Y. Chen, and F. Nori, Nat. Phys. **9**, 10 (2013).
[13] S. Huelga and M. Plenio, Contemp. Phys. **54**, 181 (2013).
[14] M. B. Plenio and S. F. Huelga, New J. Phys. **10**, 113019 (2008).
[15] F. Caruso, A. W. Chin, A. Datta, S. F. Huelga, and M. B. Plenio, J. Chem. Phys. **131**, 105106 (2009).
[16] A. W. Chin, J. Prior, R. Rosenbach, F. Caycedo-Soler, S. F. Huelga, and M. B. Plenio, Nat. Phys. **9**, 113 (2013).
[17] A. Ishizaki, T. R. Calhoun, G. S. Schlau-Cohen, and G. R. Fleming, Phys. Chem. Chem. Phys. **12**, 7319 (2010).
[18] S. Jang, Y.-C. Cheng, D. R. Reichman, and J. D. Eaves, J. Chem. Phys. **129**, 101104 (2008).
[19] S. Jang, J. Chem. Phys. **131**, 164101 (2009).
[20] D. P. S. McCutcheon, N. S. Dattani, E. M. Gauger, B. W. Lovett, and A. Nazir, Phys. Rev. B **84**, 081305 (2011).
[21] E. N. Zimanyi and R. J. Silbey, Phil. Trans. R. Soc. A **370**, 3620 (2012).
[22] A. Ishizaki and G. R. Fleming, J. Chem. Phys. **130**, 234111 (2009).
[23] J. Strumpfer and K. Schulten, J. Chem. Phys. **131**, 225101 (2009).
[24] A. Ishizaki and G. R. Fleming, Proc. Natl. Acad. Sci. USA **106**, 17255 (2009).
[25] G.-Y. Chen, N. Lambert, C.-M. Li, Y.-N. Chen, and F. Nori, Phys. Rev. E **88**, 032120 (2013).
[26] E. J. G. Peterman, T. Pullerits, R. van Grondelle, and H. van Amerongen, J. Phys. Chem. B **101**, 4448 (1997).
[27] E. J. G. Peterman, H. van Amerongen, R. van Grondelle, and J. P. Dekker, Proc. Natl. Acad. Sci. USA **95**, 6128 (1998).
[28] M. Wendling, T. Pullerits, M. A. Przyjalgowski, S. I. E. Vulto, T. J. Aartsma, R. van Grondelle, and H. van Amerongen, J. Phys. Chem. B **104**, 5825 (2000).
[29] A. Rivas, S. F. Huelga, and M. B. Plenio, Phys. Rev. Lett. **105**, 050403 (2010).
[30] U. Ermler, G. Fritzsch, S. K. Buchanan, and H. Michel, Structure **2**, 925 (1994).
[31] A. Zouni, H.-T. Witt, J. Kern, P. Fromme, N. Krauss, W. Saenger, and P. Orth, Nature **409**, 739 (2001).
[32] K. N. Ferreira, T. M. Iverson, K. Maghlaoui, J. Barber, and S. Iwata, Science **303**, 1831 (2004).
[33] R. E. Fenna and B. W. Matthews, Nature **258**, 573 (1975).
[34] Y.-F. Li, W. Zhou, R. E. Blankenship, and J. P. Allen, J. Mol. Biol. **271**, 456 (1997).
[35] J. Koepke, X. Hu, C. Muenke, K. Schulten, and H. Michel, Structure **4**, 581 (1996).
[36] X. Hu, A. Damjanović, T. Ritz, and K. Schulten, Proc. Natl. Acad. Sci. USA **95**, 5935 (1998).
[37] D. Beljonne, C. Curutchet, G. D. Scholes, and R. J. Silbey, J. Phys. Chem. B **113**, 6583 (2009).
[38] M. Sarovar, A. Ishizaki, G. R. Fleming, and K. B. Whaley, Nat. Phys. **6**, 462 (2010).
[39] A. Nazir, Phys. Rev. Lett. **103**, 146404 (2009).
[40] K. J. van Wijk, Plant Physiol. Biochem. **42**, 963 (2004).
[41] G. Friso, L. Giacomelli, A. J. Ytterberg, J.-B. Peltier, A. Rudella, Q. Sun, and K. J. van Wijk, Plant Cell **16**, 478 (2004).
[42] T. Kleffmann, M. Hirsch-Hoffmann, W. Gruissem, and S. Baginsky, Plant Cell Physiol. **47**, 432 (2006).
[43] J. Pieper, J. Voigt, and G. J. Small, J. Phys. Chem. B **103**, 2319 (1999).
[44] V. I. Novoderezhkin and R. van Grondelle, Phys. Chem. Chem. Phys. **12**, 7352 (2010).
[45] H.-P. Breuer, E.-M. Laine, and J. Piilo, Phys. Rev. Lett. **103**, 210401 (2009).
[46] M. Wolf and J. Cirac, Comm. Math. Phys. **279**, 147 (2008).
[47] M. M. Wolf, J. Eisert, T. S. Cubitt, and J. I. Cirac, Phys. Rev. Lett. **101**, 150402 (2008).
[48] A. Jamiołkowski, Rep. Math. Phys. **3**, 275 (1972).
[49] M.-D. Choi, Linear Algebra Appl. **10**, 285 (1975).
[50] W. K. Wootters, Phys. Rev. Lett. **80**, 2245 (1998).